hybridization procedure are largely avoided. There is good preservation of tissue and sections can be treated with histological stains after the hybridization procedure. Concurrent with these studies, Dubensky et al.[24] have recently detected DNA and RNA in organs of mice following polyoma and vesicular stomatitis virus infections. Finally, preliminary results indicate that LCMV antigens can be detected in mouse sections using immunological reagents. Hence, it is now possible to detect expression of viral RNA and protein while maintaining suitable morphology for detailed study at the whole-animal level.

1. Southern, E. M. J. molec. Biol. 98, 503–517 (1975).
2. Chow, L. T., Gelinas, R. E., Broker, T. R. & Roberts, R. J. Cell 12, 1–8 (1977).
3. Berk, A. J. & Sharp, P. A. Proc. natn. Acad. Sci. U.S.A. 75, 1274–1278 (1978).
4. Sim, G. K. et al. Cell 18, 1303–1316 (1979).
5. Haase, A. T., Ventura, P., Gibbs, C. J. & Tourtellotte, W. W. Science 212, 672–675 (1981).
6. Rock, D. L. & Fraser, N. W. Nature 302, 523–525 (1983).
7. Benditt, E. P., Barrett, T. & McDougall, J. K. Proc. natn. Acad. Sci. U.S.A. 80, 6386–6389 (1983).
8. Blum, H. E. et al. Proc. natn. Acad. Sci. U.S.A. 80, 6685–6688 (1983).
9. Kafatos, F. C., Jones, C. W. & Efstratiadis, A. Nucleic Acids Res. 7, 1541–1552 (1979).
10. Brigati, D. J. et al. Virology 126, 32–50 (1983).
11. Traub, E. J. exp. Med. 63, 847–862 (1936).
12. Hotchin, J. Cold Spring Harb. Symp. quant. Biol. 27, 479–499 (1962).
13. Lehmann-Grube, F. Virol. Monogr. 10, 1–173 (1971).

14. Buchmeier, M. J., Welsh, R. M., Dutko, F. J. & Oldstone, M. B. A. Adv. Immun. 30, 275–331 (1980).
15. Pedersen, I. R. Nature, new Biol. 234, 112–114 (1971).
16. Rawls, W. E. & Leung, W-C. Compreh. Virol. 14, 157–192 (1979).
17. Southern, P. J. & Oldstone, M. B. A. in Segmented Negative Strand Viruses (eds Bishop, D. H. L. & Compans, R. W.) 59–64 (Academic, New York, 1984).
18. Rigby, P. W. J., Dieckmann, M., Rhodes, C. & Berg, P. J. molec. Biol. 113, 237–251 (1977).
19. Oldstone, M. B. A., Southern, P., Rodriguez, M. & Lampert, P. Science 224, 1440–1443 (1984).
20. Huang, A. S. & Baltimore, D. Nature 226, 325–327 (1970).
21. Holland, J. et al. Science 215, 1577–1585 (1982).
22. Hu, N-t. & Messing, J. Gene 17, 271–277 (1982).
23. Green, M. R., Maniatis, T. & Melton, D. A. Cell 32, 681–694 (1983).
24. Dubensky, T. W., Murphy, F. A. & Villarreal, L. P. J. Virol. 50, 779–783 (1984).
25. Nelson, J. A., Fleckenstein, B., Galloway, D. A. & McDougall, J. K. J. Virol. 43, 83–91 (1982).
26. Chirgwin, J. M., Przybyla, A. E., MacDonald, R. J. & Rutter, W. J. Biochemistry 18, 5294–5299 (1979).
27. Thomas, P. S. Proc. natn. Acad. Sci. U.S.A. 77, 5201–5205 (1980).

Serine- and threonine-specific protein kinase activities of purified gag–mil and gag–raf proteins

Karin Moelling*, Barbara Heimann*, Peter Beimling*, Ulf R. Rapp† & Thomas Sander*

* Max-Planck-Institut für Molekulare Genetik, Abt. Schuster, Ihnestrasse 63, D-1000 Berlin 33 (West), FRG
† Laboratory of Viral Carcinogenesis, National Cancer Institute, Frederick Cancer Research Facility, Frederick, Maryland 21701, USA

Retroviruses carry cell-derived oncogenes (v-onc) that have the potential to transform cells in culture and induce tumours in vivo[1,2]. One of the few carcinoma-inducing viruses is the acutely transforming retrovirus MH2 (refs 2, 3), which carries the putative oncogene v-mil and the known oncogene v-myc (refs 4–6). Recently, a high degree of homology was discovered between v-mil and v-raf (ref. 7), the transforming gene of the murine retrovirus 3611 murine sarcoma virus (MSV)[8], whereas homology to v-src is low[9]. Both viruses express their oncogenes as the gag-fusion polyproteins[6,10] p100$^{gag-mil}$ and p75$^{gag-raf}$ (of respective relative molecular mass (M_r) 100,000 and 75,000), while the myc oncogene of MH2 is expressed by means of a subgenomic messenger RNA[11]. We have recently demonstrated that p100$^{gag-mil}$ is not a nuclear protein[6]. Here we report that purified p100$^{gag-mil}$ and p75$^{gag-raf}$ exhibit protein kinase activities in vitro which, in contrast to the src-related p130$^{gag-fps}$ of Fujinami sarcoma virus (FSV)[12] and all other characterized oncogene-encoded protein kinases, phosphorylate serine and threonine but not tyrosine. Both types of protein kinases phosphorylate lipids in vitro.

Previously reported protein kinase studies of p75$^{gag-raf}$ have involved immunoprecipitation analyses. We have recently been able to recover highly purified and enzymatically active p130$^{gag-fps}$ protein kinase from FSV-transformed cells[13–16] (P. Donner et al., manuscript in preparation), and have applied our protocol here to investigate whether p100$^{gag-mil}$ and p75$^{gag-raf}$ possess protein kinase activity. Immunoaffinity purification of p100$^{gag-mil}$ and p130$^{gag-fps}$ was performed by using monoclonal immunoglobulins (IgG) against p19, the amino-terminus of the gag portion[17]. ^{35}S-methionine-labelled cellular extracts of FSV- and MH2-transformed cells were applied to the columns to purify p100$^{gag-mil}$ and p130$^{gag-fps}$ (Fig. 1). As a control, p110$^{gag-myc}$ from MC29-transformed quail fibroblasts was also purified

(p110, Fig. 1). Purification efficiency by this procedure is about 3,000-fold[17].

p75$^{gag-raf}$ carries a murine viral gag protein and cannot be isolated using the column described above. Therefore, IgG specific for the murine viral structural protein p30 was purified from polyvalent anti-p30 rabbit serum and used to set up an immunoaffinity column. p75$^{gag-raf}$ was isolated from ^{35}S-methionine-labelled 3611 MSV-transformed rat fibroblasts. 3611 MSV codes for a doublet consisting of a glycoprotein of M_r 90,000 (gp90$^{gag-raf}$) and p75$^{gag-raf}$ (ref. 8). Figure 1 shows the purified proteins. Two additional bands were detected which have been observed previously in immunoprecipitates and are considered to be gag-processing proteins[10].

Both types of immunoaffinity columns were treated with 0.5% SDS after elution of the ^{35}S-methionine-labelled gag-fusion proteins so as to isolate possible residual proteins remaining on the immunobeads. No such proteins were detected (data not shown). Similarly, when aliquots of the immunoaffinity columns loaded with the ^{35}S-methionine-labelled gag-fusion proteins were analysed by polyacrylamide gel electrophoresis in analogy to the protein kinase experiments described below, no protein contamination was detected (data not shown).

The proteins recovered from ^{35}S-methionine-labelled cellular extracts showed no protein kinase activity. Enzymatically active proteins were recovered only from unlabelled cellular lysates applied to the immunoaffinity columns using a modified approach. Instead of being eluted from the columns, the proteins were allowed to remain attached to the immunobeads for protein kinase assay. The assays used 10 mM Mg^{2+} and 10 mM Mn^{2+} as divalent cations (Fig. 2); the optimum ion concentration has been determined to be 10 mM Mn^{2+} in all cases (data not shown). Autophosphorylation of p100$^{gag-mil}$, p75$^{gag-raf}$, and p130$^{gag-fps}$ was detected, but no autophosphorylation occurred with gp90$^{gag-raf}$ or p110$^{gag-myc}$. In the case of 3611, two additional bands of lower relative molecular mass were phosphorylated. Preliminary evidence indicates that these bands are the result of proteolytic processing[10]. The absence of protein kinase from MC29-transformed quail fibroblasts after even longer exposure times indicates that the p100$^{gag-mil}$ protein kinase activity is not of normal quail cell origin.

An additional control experiment was performed to exclude the possibility that the serine/threonine protein kinase was of rat cell origin. 3611 MSV cells were passed over an anti-p19 column as a nonspecific IgG-containing column. No protein kinase activity was detected (Fig. 2a, control). The autophosphorylation reactions were standardized to identical protein
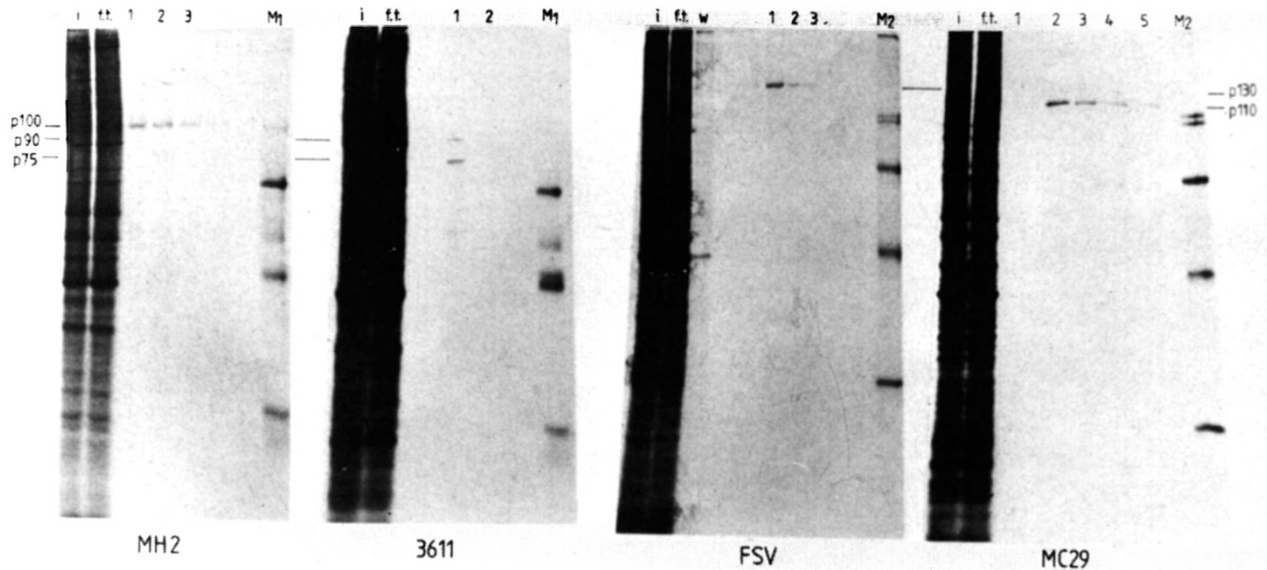
MH2   3611   FSV   MC29

Fig. 1 Immunoaffinity purification of p100$^{gag\text{-}mil}$, p75$^{gag\text{-}raf}$, p130$^{gag\text{-}frs}$, and p110$^{gag\text{-}myc}$ proteins. i, Input; f.t. flow through; lanes 1–5, eluted fractions; M_1, M_2, size markers (M_r ($\times 10^{-3}$) from top to bottom: M_1, 92, 69, 55, 46, 30; M_2, 92, 69, 46, 30). Specific activities of the eluted proteins were: p90/75$^{gag\text{-}raf}$, 8×10^4 cpm μg^{-1}; p130$^{gag\text{-}fps}$, 5×10^4 c.p.m. μg^{-1}; p100$^{gag\text{-}mil}$, 3.6×10^4 c.p.m. μg^{-1}; p110$^{gag\text{-}myc}$, 6×10^4 c.p.m. μg^{-1}.
Methods: The cell lines used in this study were MH2-transformed non-producer quail fibroblasts[6], 3611 MSV-transformed non-producer rat fibroblasts[8], FSV-transformed rat fibroblasts[12] and MC29-transformed non-producer quail fibroblasts[17]. 5×10^7 cells of each of the cell types were labelled with ^{35}S-methionine (250 μCi ml^{-1}) at 80% confluency for 2 h, lysed with 10 ml RIPA buffer (50 mM Tris-HCl pH 7.2, 150 mM NaCl, 0.1% SDS, 1% deoxycholate, 1% Triton X-100), 10 U ml^{-1} Trasylol, centrifuged (10,000 r.p.m., 30 min, 4 °C) and applied to immunoaffinity columns containing IgG against the murine viral protein p30 in the case of 3611, and against p19 for the other cell types. The anti-p30 column was prepared as follows: p30 was isolated by phosphocellulose column chromatography from 50 mg of MSV using elution conditions described elsewhere[23]. Isolated p30 (1 mg) was coupled to activated CH-Sepharose 4B (Pharmacia). Goat anti-p30 serum (10 ml) was passed over the p30 column and specific IgG recovered. This anti-p30 IgG (2 mg) was then coupled to protein A–Sepharose 4B (0.2 g) as described elsewhere[17] and used as anti-p30 immunoaffinity column. The anti-p19 immunoaffinity column has been described elsewhere[17]. After extensive washing, the purified proteins were eluted with citric acid buffer, pH 3.5, which was neutralized immediately. The eluted proteins (30 μl per 2 ml of each fraction) were analysed by gel electrophoresis and autoradiography.

Fig. 2 *a*, Protein kinase assay of purified proteins. *b*, Phosphoamino acid analysis.
Methods: *a*, 2×10^7 cells of MH2-, 3611-, FSV- and MC29-transformed non-producer fibroblast lines each were lysed with RIPA buffer in the presence of 1 mM dithiothreitol, centrifuged (10,000 r.p.m., 30 min, 4 °C) and applied to immunoaffinity columns (200 μl of packed beads each) as described in Fig. 1 legend. 3611 lysates were also applied to an anti-p19 immunoaffinity column (3611 control). The columns were washed extensively[17]. Instead of eluting the proteins from the columns, they remained immobilized on the beads and were distributed to reaction tubes for further analysis. Protein kinase activities were tested in a total volume of 50 μl containing 50 mM Tris-HCl pH 7.5, 50 mM NaCl, 1 mM dithiothreitol, supplemented with 10 mM MgCl$_2$ (Mg) or 10 mM MnCl$_2$ (Mn). 5 μl enzyme-coupled beads were used per reaction. Incubation time was 10 min at 37 °C. 20 μCi of [γ-^{32}P]ATP (3,000 Ci mmol^{-1}) were used per assay. Reactions were terminated by the addition of four-

a

Mg Mn   Mg Mn   Mg Mn   Mg Mn   Mg Mn

— p130
— p110
— p100
— p90
— p75

MH2   3611   FSV   MC29   3611
2 h   6 h   1 h   3 days   control
                                 8 days

b

MH2   3611   FSV

— ser
— thr
— tyr

fold concentrated sample buffer[17] for SDS-polyacrylamide gel electrophoretic analysis. Samples were treated for 1 min at 100 °C and applied directly to the gels. The gels were dried and exposed for autoradiography for the indicated periods of time. *b*, The autophosphorylated proteins were cut out of the gels, eluted and processed for phosphoamino acid analysis as reported previously[18]. Exposure time was 3–5 days at −70 °C using intensifier screens.
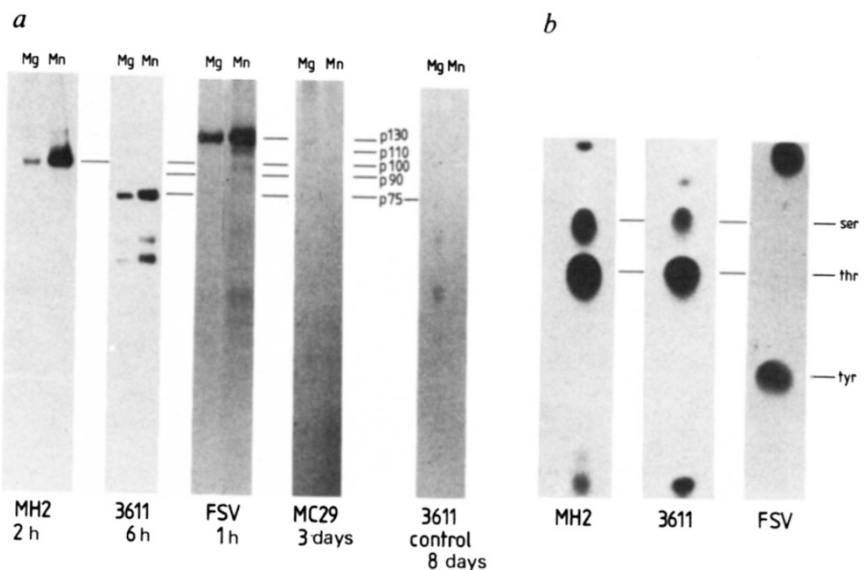
contents of the lysate inputs. The immunoaffinity columns contained excess IgG and bound all available gag-fusion proteins. Based on these findings, we determined the radioactivity incorporated into the individual bands and found that p130$^{gag\text{-}fps}$ incorporated fivefold more radioactivity than did p100$^{gag\text{-}mil}$ or p75$^{gag\text{-}raf}$.

The phosphoamino acid content of the autophosphorylated proteins was determined[18]. Figure 2*b* shows that p100$^{gag\text{-}mil}$ and p75$^{gag\text{-}raf}$ are not tyrosine-specific protein kinases like p130$^{gag\text{-}fps}$, but phosphorylate serine and threonine instead. As both

p130$^{gag\text{-}fps}$ and p75$^{gag\text{-}raf}$ originate from rat cells[12], the differences in amino acid phosphorylation rule out protein kinase contamination by rat cells.

p75$^{gag\text{-}raf}$ lacks the tyrosine acceptor site found in src[19]. It was therefore important to analyse the amino acid specificities of p100$^{gag\text{-}mil}$ and p75$^{gag\text{-}raf}$ not only in autophosphorylation reactions but also with exogenous substrates. For this we used rabbit muscle actin, calf thymus arginine- and lysine-rich histones, chicken H5, and phosvitin; casein was not used because of its high degree of autophosphorylation. The three protein kinases
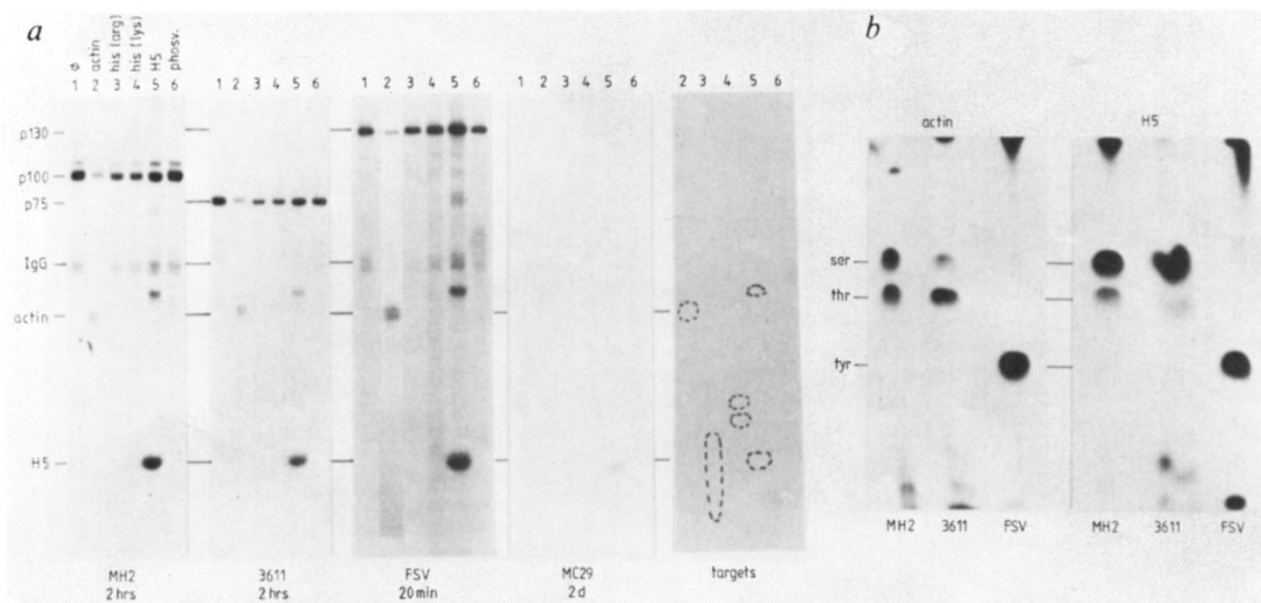
Fig. 3 Phosphorylation of substrates *in vitro*. *a*, Immunobead-immobilized enzymes were tested for their ability to phosphorylate exogenous substrates (5 µg each, all from Sigma) *in vitro*. Protein kinase assays were performed as described in Fig. 2 legend in the presence of 10 mM MnCl$_2$. Lanes 1, no substrate; 2, actin; 3, histones, arginine-rich [his(arg)]; 4, histones, lysine-rich [his(lys)]; 5, chicken histone H5; 6, phosvitin. For control, all substrates were tested for autophosphorylation in the absence of kinases. Exposure time was as indicated using intensifier screens at −70 °C. The dotted circles indicate where the substrates migrated as determined by Coomassie blue staining. *b*, Phosphoamino acid analysis of the two substrates actin and H5 phosphorylated by MH2, 3611 and FSV protein kinases. The phosphoproteins were cut out of the gel shown in *a* and processed as described previously[18]. For exposure time, see Fig. 2*b* legend.
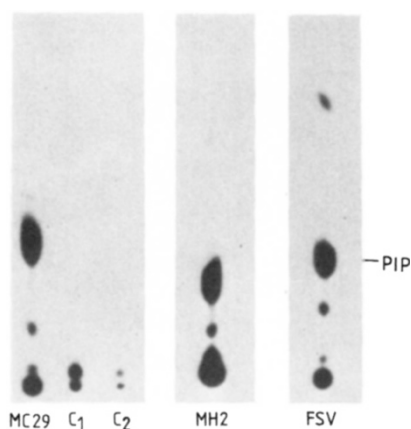

Fig. 4 TLC analyses of lipids radiolabelled with [γ-^{32}P]ATP. Immunobead-immobilized protein kinases from MH2-, FSV- and MC29-transformed cells were incubated with detergent-treated L-α-phosphatidylinositol 4-monophosphate. Details of the conditions have been published elsewhere[14]. Abbreviation: PIP, L-α-phosphatidylinositol; C$_1$, control in which lipic was omitted; C$_2$, control in which protein was omitted. PIP marker was co-chromatographed and traced by fluorescent light. Exposure time was 3 days at −70 °C using intensifier screens.

phosphorylated histone H5 and actin, but phosphorylation of the other substrates was undetectable (Fig. 3*a*). When phosphoamino acid analysis was performed with the phosphorylated actin and H5 target molecules (Fig. 3*b*), p100$^{gag-mil}$ and p75$^{gag-raf}$ produced serine and threonine phosphorylation, while p130$^{gag-fps}$ phosphorylated tyrosine. Some IgG also became phosphorylated. Actin seemed to inhibit autophosphorylation, while cyclic AMP inhibited all three protein kinase activities at concentrations ranging from 5 µM to 0.5 mM (data not shown).

The recent finding that two src-related tyrosine protein kinases show lipid-phosphorylating activity[20,21] raised the question of whether the protein kinases described here, although lacking tyrosine specificity, are also lipid kinases. Figure 4 shows that p100$^{gag-mil}$ and p130$^{gag-fps}$ indeed phosphorylate lipids *in vitro*. However, MC29 and normal quail cells processed by anti-p19 immunoaffinity chromatography resulted in similar levels of lipid phosphorylation under identical assay conditions (see MC29, Fig. 4).

Our results describe for the first time the presence of a serine/threonine protein kinase activity in two purified oncogene protein products. This activity is absent from quail and rat cell lines transformed by two other oncogenes, indicating that the kinase is not of cellular origin. Our results demonstrate that tyrosine phosphorylation can no longer be considered as a definitive property of oncogene-specific protein kinases. The recently observed lipid phosphorylation through the action of src[20] and ros[21] oncogenes does not appear to be an intrinsic property of the protein kinases described here since similar levels of activity were also found associated with p110$^{gag-myc}$ and normal cell controls. Phosphorylation of lipids or proteins as potential target molecules needs further evaluation. Indirect evidence suggests that the serine/threonine protein kinases described here may not be unique to mil/raf but may also be characteristic of the mos oncogene[22].

and S. Sukrow for technical assistance, and Dr H. Hanafusa for supplying FSV-transformed rat cell line. Dr H. Dieringer contributed stimulating discussions on the lipid assays.

1. Bishop, J. M. A. Rev. Biochem. 52, 301-354 (1983).
2. Beard, J. W. in Viral Oncology (ed. Klein, G.) 55-87 (Raven, New York, 1980).
3. Alexander, R. W., Moscovici, C. & Vogt, P. K. J. natn. Cancer Inst. 62, 359-366 (1979).
4. Jansen, H. W., Patschinsky, T. & Bister, K. J. Virol. 48, 61-73 (1983).
5. Kan, N. C. et al. Proc. natn. Acad. Sci. U.S.A. 80, 6566-6570 (1983).
6. Bunte, T., Greiser-Wilke, I. & Moelling, K. EMBO J. 2, 1087-1092 (1983).
7. Jansen, H. W. et al. Nature 307, 281-284 (1984).
8. Rapp, U. R. Proc. natn. Acad. Sci. U.S.A. 80, 4218-4222 (1983).
9. Sutrave, P. et al. Nature 309, 85-88 (1984).
10. Rapp, U. R., Reynolds, F. H. & Stephenson, J. R. J. Virol. 45, 914-924 (1983).
11. Pachl, C., Biegalke, B. & Linial, M. J. Virol. 45, 133-139 (1983).
12. Feldman, R. A., Hanafusa, T. & Hanafusa, H. Cell 22, 757-765 (1980).
13. Moelling, K. Adv. Cancer Res. 43 (in the press).
14. Moelling, K., Owada, M. K., Greiser-Wilke, I., Bunte, T. & Donner, P. J. cell. Biochem. 20, 63-69 (1982).
15. Moelling, K., Bunte, T., Greiser-Wilke, I., Donner, P. & Pfaff, H. in Cancer Cells Vol. 2, 173-180 (Cold Spring Harbor Laboratory, New York, 1984).
16. Moelling, K., Donner, P., Bunte, T. & Greiser-Wilke, I. Contr. Oncol. 19, 35-43 (1984).
17. Donner, P., Greiser-Wilke, I. & Moelling, K. Nature 296, 262-266 (1982).
18. Sefton, B. M., Hunter, T., Beemon, K. & Eckardt, W. Cell 20, 807-816 (1980).
19. Mark, G. E. & Rapp, U. R. Science 224, 285-289 (1984).
20. Sugimoto, Y., Whitman, M., Cantley, L. C. & Erikson, R. L. Proc. natn. Acad. Sci. U.S.A. 81, 2117-2121 (1984).
21. Macara, I. G., Marinetti, G. V. & Balduzzi, P. C. Proc. natn. Acad. Sci. U.S.A. 81, 2728-2732 (1984).
22. Kloetzer, W. S., Maxwell, S. A. & Arlinghaus, R. B. Proc. natn. Acad. Sci. U.S.A. 80, 412-416 (1983).
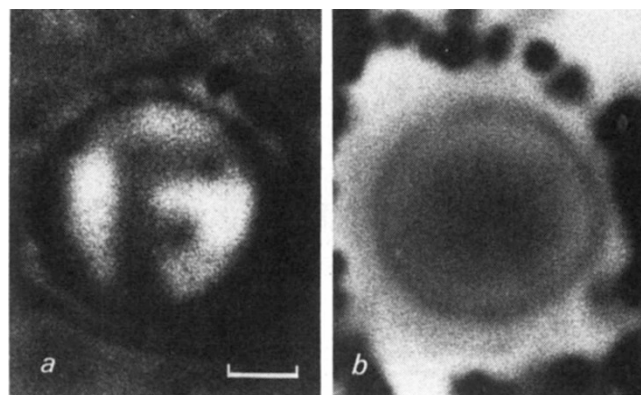23. Moelling, K., Sykora, K.-W., Dittmar, K., Scott, A. & Watson, K. F. J. biol. Chem. 254, 3738-3742 (1979).

Fig. 1 Transverse sections of the proximal region of butterfly (Heteronympha) crystalline cones, cut in a cryotome after 1 h fixation. a, An image is formed of a distant letter 'F'. The inverted image is here re-inverted by the microscope. The focal length (in this case 5.1 μm) was calculated from the relative size of the image. Sections with similar focal lengths were obtained from various different butterflies: Junonia villida (Nymphalidae), Pieris rapae (Pieridae), Zizina labradus (Lycaenidae) and Papilio aegeus (Papilionidae). b, A protein gradient revealed by binding of tolouidine blue (in Heteronympha). Scale bar, 1 μm.

Afocal apposition optics in butterfly eyes

D.-E. Nilsson*, M. F. Land* & J. Howard*

Department of Neurobiology, Research School of Biological Sciences, Australian National University, PO Box 475, Canberra, ACT 2601, Australia

In most apposition compound eyes there are two components to the optical system of the ommatidium[1,2], the cornea and the crystalline cone. The focusing power of the cornea is well documented[3,4] whereas the crystalline cone is usually regarded as a mere optical spacer[5,6]; consequently, the ommatidial optics will consist of a simple focusing lens. To the contrary, we now demonstrate the existence of a complete afocal telescope in each ommatidium of butterfly apposition eyes. The optical system is an extreme variant of that found in refracting superposition eyes, thereby providing a connection between butterflies and moths.

The apposition eye consists of optically isolated units (ommatidia) each having a lens forming an inverted image (see Fig. 1 of ref. 7). In superposition eyes, the lens systems of many ommatidia cooperate to form a superimposed erect image.

Here we measured the optical properties of the ommatidia in the eye of a common Australian nymphalid butterfly, Heteronympha merope. The focal length, f, of the cornea (posterior nodal distance) was determined by suspending a cleaned corneal cup from a hanging drop of Ringer's solution, and measuring the size of the image of a distant object viewed through the cornea; this gave a focal length of 48.6 ± 1.2 μm ($\pm$s.d., $N = 10$). The distance from the cornea to the image ($f' = nf$) is 67.3-70.7 μm. (The refractive index used here, $n = 1.42$, is an average derived from cornea (1.52), corneal process (1.34) and cone (1.41).) In sectioned material the rhabdom tips are consistently found at a depth of 70 μm, so that if the crystalline cones had no optical power, an image would be formed at the rhabdom tips. If, however, the crystalline cone acts as a lens, then the system cannot be using simple focal optics.

The crystalline cones are so small (2.5 μm wide proximally) that most measurement techniques, including interference

microscopy, are inadequate to resolve their optical structure. The method we finally used was as follows. Sections (4-8 μm) of stabilized material (1 h in 3% glutaraldehyde, 2% formaldehyde and 4% sucrose in 150 mM Na-cacodylate buffer) were cut in a cryotome at -14 °C, then examined to determine whether they formed images (see Fig. 1a). Parallel-sided sections of the cones do indeed form inverted images and behave as powerful converging lenses. As judged from the unaffected pseudopupil, the optics were not damaged by the fixation. Staining of the sections with toluidine blue[8] revealed a concentric protein gradient that is probably responsible for the focusing properties (Fig. 1b).

From the magnification of the images it was possible to work out the power ($1/f$) of sections taken at different levels along the cone. Figure 2a shows that most of the power lies in the proximal tip region; given this distribution, we were then able to trace rays through the cone by substituting each micrometre with a thin lens whose power is given by the ordinate in Fig. 2a. The results of this simulation are shown in Fig. 2b, c. Surprisingly, we found that the proximal region of the cone has exactly the right optical properties to convert the focused beam of light supplied by the cornea into a parallel beam whose diameter fits the rhabdom (2.2 μm). The weak middle region of the cone brings the converging beam to a focus ~8 μm from the proximal tip of the cone, and in that 8 μm there is the equivalent of a lens powerful enough to re-collimate the focused light into a parallel beam directed down the rhabdom. It is noteworthy that this second lens is probably the most powerful known to man (0.2 megadioptres).

The optical properties of the ommatidium as a whole are accurately modelled by one spherical surface (cornea) and two thin lenses (cone) as in Fig. 3; it has the optical form of a telescope (in fact, properly known as a keplerian telescope with a Huygens eyepiece[9]). The angular magnification is 6.4, so that rays reaching the cornea at 1° to the optical axis emerge into the rhabdom at 6.4° (Fig. 2c). Note that the field of view of an ommatidium is now not determined by the rhabdom diameter, but by the maximum angle up to which the rhabdom will act as a light guide (in geometric optics this would be the complement of the critical angle). It also follows from the telescopic design that the rhabdom tip is imaged onto the cornea, magnified 9.1 times (the angular magnification multiplied by the refractive index inside the eye); this would mean that the 2.2 μm-wide rhabdom tip fills the central 20 μm of the 25 μm-wide facet, but in the domain of waveguide optics this cut-off will not be sharp.

* Present addresses: Department of Zoology, University of Lund, Helgonavagen 3, S-223 62 Lund, Sweden (D.E.N); School of Biological Sciences, University of Sussex, Brighton BN1 9QG, UK (M.F.L.); Department of Physiology, University of Bristol Medical School, University Walk, Bristol BS8 1TD, UK (J.H.).